B. Urév and P. A. Rebinder, *Dokl. Akad. Nauk.*, **89**, 369 (1969).
(10) G. U. Stratulat, I. N. Vladavets, N. N. Serb-Serbina, and P. A. Rebinder, *Kolloid Zh.*, **32**, 765 (1970).
(11) (a) S. J. Hahn, T. Ree, and H. Eyring, *NLGI Spokesman*, (J. National Lubricating Grease Institute), **21**, 12 (1957); **23**, 129 (1959); *Ind. Eng. Chem.*, **51**, 856 (1959); (b) H. Utsugi, H. Iwasawa, and T. Ree, *Nippon Kagaku Zasshi*, **91**, 690 (1970).
(12) H. Green, *Ind. Eng. Chem., Anal. Ed.*, **14**, 575 (1942).
(13) (a) R. N. Weltmann, *NLGL Spokesman* (J. National Lubricating Grease Institute), **20**, No. 3, 34 (1956); (b) H. Utsugi, K. Kim, T. Ree and H. Eyring, *ibid*, **25**, 125 (1961).
(14) T. Ree and H. Eyring, *Rheology*, ed. by F. R. Eirich, Vol. II, p. 83, Academic Press, New York, 1958, p. 591; J. App. Phys., **26**, 793, 800 (1955).
(15) M. B. M'Ewen and M. I. Pratt, *Trans. Faraday Soc.*, **53**, 535 (1957).
(16) K. Norrish, *Discussions Faraday Soc.*, **18**, 120 (1954).
(17) H. van Olphen, *An Introduction to Clay Colloid Chemistry*, Interscience, New York, 1963, p. 301.
(18) J. L. McAtee, Jr., *Clays and Clay Minerals*, Nat. Res. Council, 5th Conf., 279-288, 1958.
(19) N. Mungan and F. W. Jessen, *Clays and Clay Minerals*, Nat. Acad. Sci. - Nat. Res. Council, 11th Conf., 283-294 (1962).
(20) S. Glasstone, K. J. Laidler and H. Eyring, *The Theory of Rate Processes*, McGraw-Hill, New York, 1941, p. 611.
(21) K. Park, *Thesis*, Department of Metallurgy, University of Utah, Salt Lake City, Utah, U. S. A., 1966.

DAEHAN HWAHAK HWOEJEE
(Journal of the Korean Chemical Society)
Vol. 15, No. 6, 1971
Printed in Republic of Korea

Effect of Electrolytes on Flow Properties of Aqueous Bentonite Suspension

Kisoon Park,* Taikyue Ree and **Henry Eyring**

Department of Chemistry, University of Utah
Salt Lake City, Utah, U. S. A.

(Received Oct. 21, 1971)

Abstract Dependence of the flow behavior of aqueous suspension of Black Hills bentonite on the concentration and the type of electrolytes was studied. The flow properties were measured with a Couette-type rotational viscometer. On addition of monovalent cations, the apparent viscosity determined from the reproducible flow curves (shear rate *vs.* shear stress) decreased followed by a rise as the ionic concentration further increased. Addition of multivalent cations (di- and tri-) resulted in the viscosity which increased to a maximum then decreased to a constant value. Anions of different charges produced essentially the same relationship between viscosity and electrolyte concentration. The flow behavior of the electrolyte-containing suspensions was rationalized in terms of the Derjaguin-Landau-Verwey-Overbeek theory of colloidal stability and the generalized theory of viscosity.

* Present Address: Union Carbide Corporation, Chemicals and Plastics Division, South Charleston, W. Va., U. S. A.

Introduction

As is true with most clay minerals, the particle shapes of montmorillonites to which bentonite clay belongs are markedly asymmetrical. Bentonite is drastically different from the other clay minerals in that it consists of thin submicroscopic flakes with high area-to-thickness ratio (as large as 100) and that it swells extensively in the presence of water.[1,2] Consequently, the relationship between its colloidal stability and flow properties is far more complex than that of any other clay suspensions.

Due to the technological importance of bentonite, particularly in drilling-fluid applications, the peptization and flocculation in relation with rheological properties of bentonite suspension have been extensively investigated.[3,4] However, the mechanism in which the electrolytes of various ionic charges influence the flow behavior of bentonite suspension is not clearly understood.

In the present work, flow properties of the moderately concentrated suspension(8-10 wt. %) containing electrolytes of various charge types were measured. The results are rationalized in terms of the repulsive function in the DLVO (Derjaguin-Landau-Verwey-Overbeek) theory of colloidal stability[5] as well as of the generalized theory of viscosity.[6]

Experiment

Preparation of the Sample The sample studied was Black Hills (Wyoming, U. S. A.) bentonite provided by the International Minerals and Chemical Corporation, Skokie, Illinois, through the Brumley-Donaldson Company, Los Angeles, California. The chemical composition was silica, 64.72%; alumina, 20.82%; iron oxide, 3.44%; titanium oxide, 0.14%; lime, 0.49%; magnesia, 2.38%; alkalis, 2.92%.

In order to prepare suspensions yielding reproducible flow data, a Cenco stirrer with a paddle of constant shape was used throughout the experiment. Three hours of mixing at 635 rpm gave a satisfactory suspension.

The suspensions containing various amounts of salt were prepared by the following procedure: a measured amount of salt solution (0.1N KCl, KI and K_2SO_4) was added to the bentonite suspension while it was stirred, then the final electrolyte concentration was adjusted by adding distilled water.

Apparatus and Procedures The apparatus used in measuring flow properties was a Couette type rotational viscometer, the details of which were given elsewhere.[7] A cylinder set having a ratio (R_b/R_c) of 0.885(R_b and R_c are the radii of the bobbin and the cup) was used. The viscometer recorded a continuous flow curve (shear rate s *vs.* shear stress f) in 37 seconds with the peak shear rate of 682 sec^{-1}. A Leeds and Northrup Speedomax Type G X-Y recorder plotted the flow curves by recording the instantaneous torque from a Statham Model G-1 transducer and the instantaneous rotational speed from a tachometer.

Experimental Results

Figure 1 represents typical flow curves of aqueous bentonite suspensions. The upward arrow indicates the "upcurve"obtained by increasing the rate of shear from zero to the maximum shear rate*, and the downward arrow indicates a "downcurve" obtained while the shear rate was decreased from the maximum to zero. By repeating the cyclic deformation, the thixotropic loop became smaller but soon reached a constant reproducible shape (the smaller loop). The reproducible loop became smaller as the concentration of the suspension decreased. Thus, below

*Shear rate on the bobbin surface.

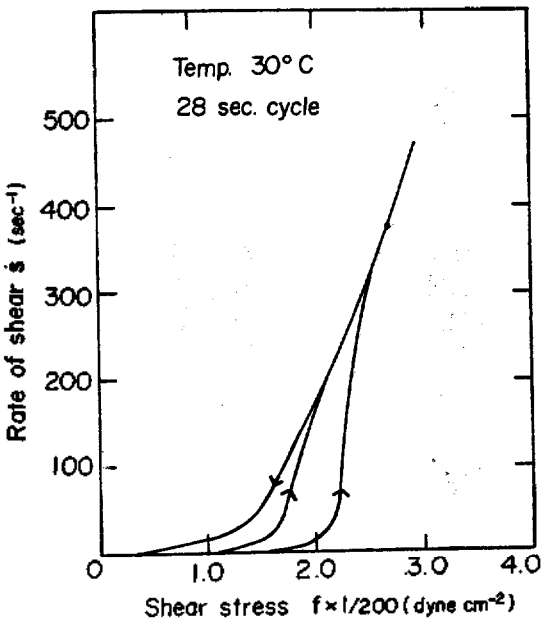

Fig. 1. Typical flow curve of 10 wt. % bentonite aqueous suspension.

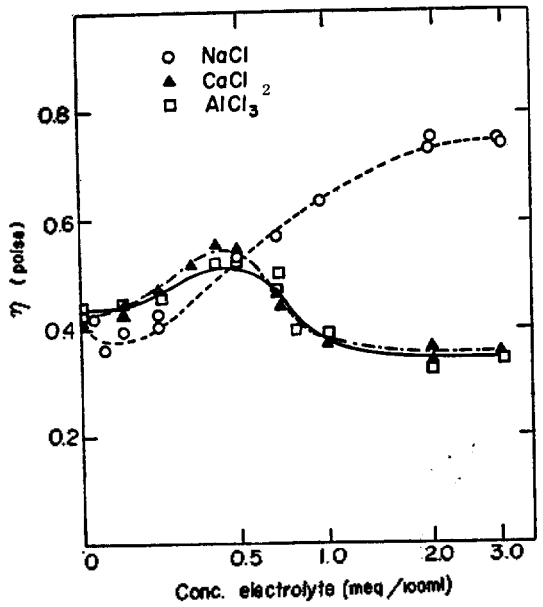

Fig. 2. Variation of apparent viscosity with electrolyte concentration for 9.0 wt. % bentonite suspension containing chloride salts of different cationic charges. All the apparent viscosities were obtained at $\dot{s}=682$ sec^{-1}, the apex $\dot{s}$ of each reproducible cyclic flow curve.

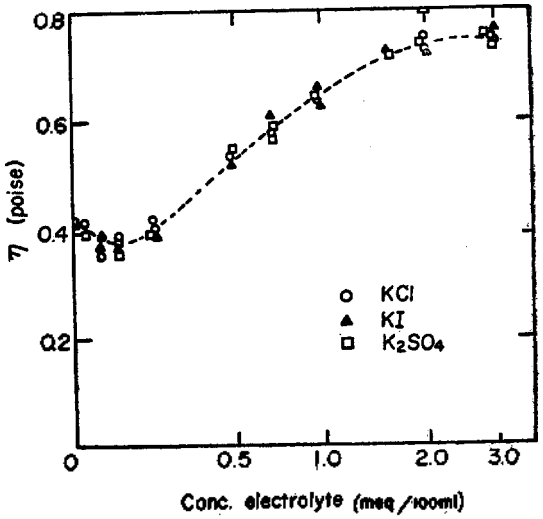

Fig. 3. Variation of apparent viscosity with electrolyte concentration for 9.0 wt. % bentonite suspension containing potassium salts of various anionic charges. All the apparent viscosities were obtained at $\dot{s}=682$ sec^{-1}, the apex $\dot{s}$ of each reproducible cyclic flow curve.

about 8 wt. %, the up and down curves almost coincided after repeated cyclic deformation. The apparent viscosity η was expressed by $\eta=f/\dot{s}$, and obtained by using the reproducible cyclic flow curves.

Shown in *Fig.* 2 are the variations of apparent viscosity with electrolyte concentration (plotted in a semilogarithmic scale) for the 9.0 wt. % suspension. All the apparent viscosities in *Fig* 2 were obtained at the apices of reproducible cyclic flow curves where the apex $\dot{s}$ for each curve was 682 sec^{-1}. Initially the apparent viscosity decreased on addition of a small amount of sodium chloride, followed by a rise when more salt was added; the viscosity value appeared to level off as the salt concentration was further increased. In contrast with the above case the suspension containing multivalent cations showed the viscosity which increased to a maximum, then decreased to a limiting value.

Fig. 3 represents the variation of apparent

viscosity of 9.0 wt. % suspension with the concentrations of the salts containing different anionic charges. Here the experimental data were obtained by the same procedure as that used for obtaining the data in *Fig.* 2. It is seen that KCl, KI and K_2SO_4 gave essentially the same relationship between the apparent viscosity and the electrolyte concentration. The dotted line is the best averaged curve for the KCl-system.

Discussion

DLVO Theory A quantitative discussion on the interparticle forces of lyophobic colloids is offered by the well-known DLVO theory.[5] The basic concept of their theory is the existence of a repulsion due to the interaction of two electric double layers and of the attraction by the London-van der Waals forces. The stability of a colloid is explained as arising from the interactions of these two forces. Based on the classical double layer theory, they deduced the following equation for the repulsive potential V_R:

$$V_R=\frac{8\epsilon k^2T^2\kappa}{\pi(\nu e)^2}\,\gamma^2\exp(-2\kappa d) \qquad (1)$$

in which κ and γ are expressed as follows:

$$\kappa=\left(\frac{s\pi n\nu^2e^2}{\epsilon kT}\right)^{\frac{1}{2}}\equiv 1/\delta \qquad (2)$$

and

$$\gamma=\frac{\exp(y_0/2)-1}{\exp(y_0/2)+1};\qquad y_0=\frac{\nu e\Psi_0}{kT}$$

Here, Ψ_0 surface potential, ν valence of ions, e electronic charge, ϵ dielectric constant of the medium, d half-distance between two plates of colloidal particles, k the Boltzman constant, T absolute temperature and n ionic concentration (no. of ions/cm^3). The reciprocal of κ, or δ is inversely proportional to the ionic valence and to the square root of the ionic con centration.

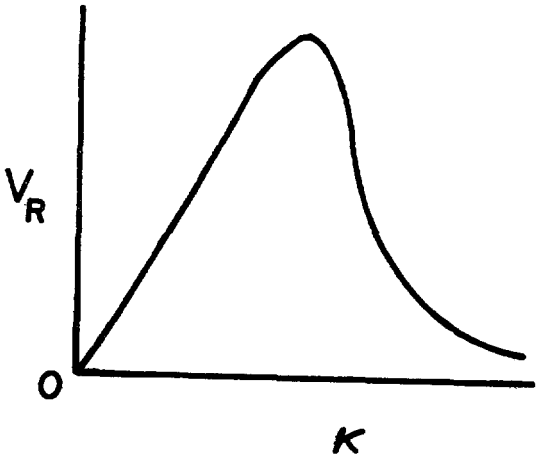

Fig. 4. The repulsive potential V_R *vs.* κ in an arbitrary scale.

Fig. 4 is a plot of the repulsive potential V_R versus κ on an arbitrary scale [Eq (1)]. One sees that V_R has a maximum at a certain value of κ. The attraction potential V_A is given by the equation,

$$V_A=-\frac{\pi q^2\lambda}{48}\left[\frac{1}{d^2}+\frac{1}{(d+\sigma)^2}-\frac{2}{(d+\sigma/2)^2}\right] \qquad (3)$$

where d is the half-distance between two parallel plates; σ, the thickness of the plate; q, the number of atoms per 1 cm^3 of the plate and λ is a factor involved in the London formula, $V=\lambda/r^6$.

The effect of electrolyte on the flow behavior of bentonite suspension will be explained later in terms of the DLVO theory.

Flow Equation for Bentonite Suspension The electric double layer of sodium bentonite, *e. g.*, Black Hills type which exhibits a high cation exchange capacity, is due to the well developed negative surface charge produced by

an isomorphous substitution of tetravalent Si^{+4} by trivalent Al^{+3} in the crystalline structure. In the stack of unit layers which form a platelike particle, the exchangeable cations are located on each side of the unit layer; hence, they are present not only on the external surfaces of the particle but also in between the unit layers. In the presence of water, the compensating cations on the layer surfaces can be exchanged by other cations, and some of the adsorbed compensating ions act as the counter ions in the diffuse layer. Consequently, the bentonite in contact with water swells spontaneously and the volume increases to as much as several hundred percent.[3] As it swells, the platelike particles separate into individual layers to a large extent making the "card-house" structure. The cardhouse structure is visualized as a system of parallel plates held together by cross-linking faces to edges leading to a voluminous scaffolding structure. Crosslinking forces associated with the edge-to-face bonding are electrostatic attraction between the oppositely charged edges and faces as well as van der Waals' attractive force. Though the edge-to-edge interaction also contributes to the formation of card-house structure, the interaction of this type is much weaker than the edge-to-face interaction which arises mainly from the dissimilar charges on the edges and the surfaces.

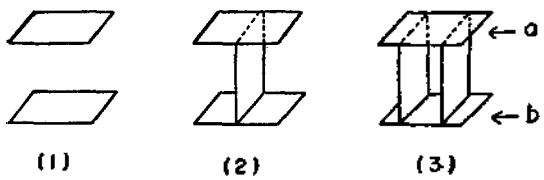

Fig. 5. Schematic representation of flow units in bentonite suspension.

In a paper[8], we assumed that there are three kinds of flow units in a shear surface of bentonite suspension as depicted in *Fig.* 5. In type 1, two flakes of bentonite flow past each other lubricated by the fluid in between. In types 2 and 3, the two parallel flakes are physically bonded together by one and two flakes of bentonite. Furthermore, units of type 2 break easily forming type 1 units by the shear stress. Type 3 units rarely break, and when they do, recover quickly so that their concentration is unaffected by the rate of flow. The scaffolding structure is assumed to be an assembly of these three kinds of units.

A non-Newtonian system is considered to be composed of flow units of different relaxation times in the generalized theory of flow.[6] The viscosity η defined as $f/\dot{s}$ is expressed by the following equation;

$$\eta=\sum_{n=1}^{n}\frac{X_n\beta_n}{\alpha_n}\ \frac{\sinh^{-1}\beta_n\dot{s}}{\beta_n\dot{s}} \tag{4}$$

where β_n is a quantity proportional to the relaxation time of the nth type flow unit, X_n the fraction of the area occupied by the nth type units on a shear surface, and α_n is a parameter, the reciprocal of which is proportional to the shear modulus. Here the quantities β_n and $1/\alpha_n$ are defined as the intrinsic relaxation time and the intrinsic shear modulus of type n unit, respectively.

For the reproducible downcurve, two types of flow units of bentonite particles, a Newtonian type and a non-Newtonian type, were introduced[8] to describe the variation of η with $\dot{s}$ along the downcurves. The equation for bentonite suspension is then written as;

$$\eta=\frac{X_1'\beta_1}{\alpha_1}+\frac{X_3\beta_3}{\alpha_3}\ \frac{\sinh^{-1}\beta_3\dot{s}}{\beta_3\dot{s}} \tag{5}$$

where, the Newtonian unit corresponds to type 1 while the non-Newtonian unit is represented by type 3. Park and Ree[8] described the thixotropic hysteresis loop of bentonite suspension by considering the transition between type 2 units

and type 1 units, and it was assumed that type 2 units completely transform to type 1 at the apices of upcurves under experimental conditions which were similar to the present work.

Equation (5) is not accurately applicable to the whole range of downcurves, since it was found[8] that the recovery of the broken type 2 units occurs appreciably when $\dot{s} < 200$ sec^{-1}. Thus, the application of Eq. (5) was limited to the downcurve above $\dot{s}=200$ sec^{-1} treating the quantities $X_1'\beta_1/\alpha_1$ and X_3/α_3 as constants.*

The procedure for finding the parametric values in Eq. (5) was as follows: For a downcurve, a plot of η versus $\dot{s}$ (>200 sec^{-1}) was first made, then the η values were extrapolated to $\dot{s}=0$. Since $(\sinh^{-1}\beta_3\dot{s})/\beta_3\dot{s}$ approaches unity at $\dot{s}=0$, the extrapolated value of η becomes

$$\eta(\dot{s}=0) = \frac{X_1'\beta_1}{\alpha_1} + \frac{X_3\beta_3}{\alpha_3} \qquad (6)$$

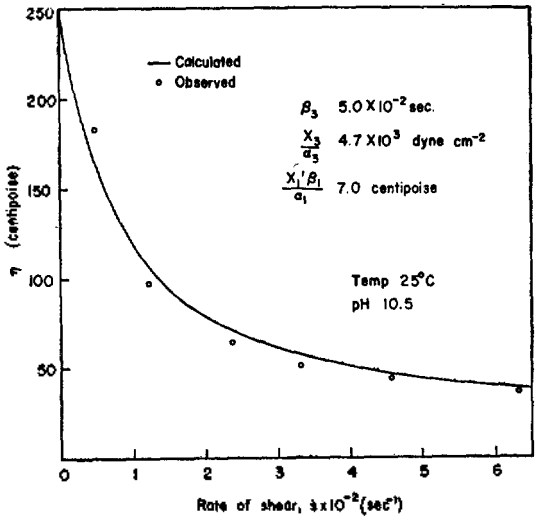

Fig. 6. Comparison of observed and calculated apparent viscosities for 8.0 wt. % bentonite suspension. The experimental data were obtained from the downcurve above $\dot{s}=200$ sec^{-1} of the reproducible cyclic flow curve.

*The quantity X_1' in Eq. (5) is considered to be the sum of X_1 and X_2 defined previously, and it defines the area occupied by all type 1 units including the one transformed from type 2 units.

Table I* Typical values of flow parameters of 9.5 wt. % bentonite suspension containing various amounts of sodium chloride.

Conc. NaCl (meq./100 ml)	$(X_1'\beta_1/\alpha_1)\times10^2$ (poise)	X_3/α_3 (dyne cm^{-2})	β_3 (sec.)
0.00	4.0	44.38	0.265
0.10	3.0	44.05	0.148
0.25	4.0	49.90	0.304
0.50	7.0	64.10	0.466
1.00	8.0	70.79	0.856
2.00	10.0	78.76	1.50
3.00	10.0	80.00	1.46

*All the parametric values were obtained from the downcurves above $\dot{s}=200$ sec^{-1} of the reproducible cyclic flow curves.

The values of β_3 were selected so that the plot of η versus $(\sinh^{-1}\beta_3\dot{s})/\beta_3\dot{s}$ gave a straight line. The value of $X_1'\beta_1/\alpha_1$ was found from the intercept and the value of X_3/α_3 from the slope by using the value of β_3 found.

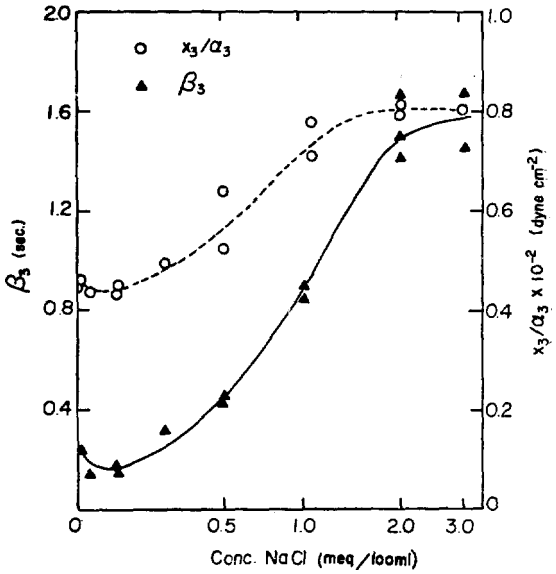

Fig. 7. Dependence of parametric values of β_3 and X_3/α_3 on NaCl concentration for 9.5 wt. % bentonite suspension. The parametric values were obtained by analyzing the downcurve above $\dot{s}=200$ sec^{-1} of each reproducible cyclic flow curve.

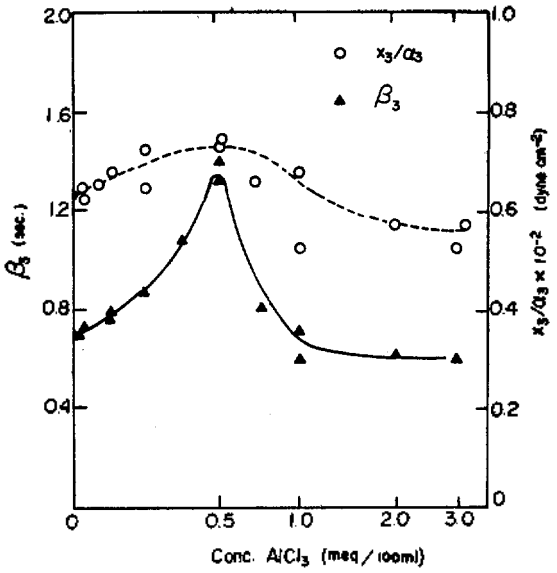

Fig. 8. Dependence of parametric values of β_3 and X_3/α_3 on $AlCl_3$ concentration for 9.0 wt. % bentonite suspension. The parametric values were obtained by analyzing the downcurve above $\dot{s}=200$ sec^{-1} of each reproducible cyclic flow curve.

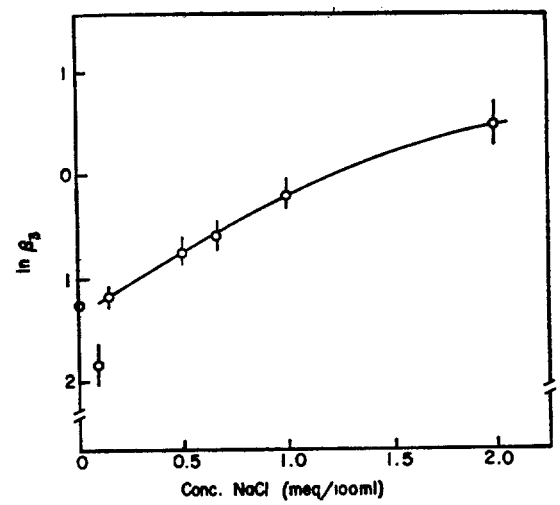

Fig. 9. Ln β_3 *vs.* sodium chloride concentration for 9.5 wt. % bentonite suspension.

Fig. 6 represents an example of the plot of η *vs.* $\dot{s}$ for an 8 wt. % suspension where the experimental and calculated data are compared.

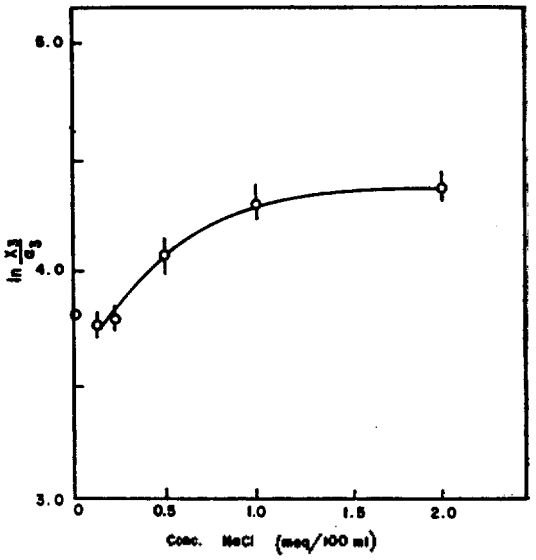

Fig. 10. Ln X_3/α_3 *vs.* sodium chloride concentration for 9.5 wt. % bentonite suspension.

The parametric values appear on the diagram. *Table* I summarizes typical parametric values for the 9.5 wt. % suspensions containing various amounts of sodium chloride. The dependence of X_3/α_3 and β_3 on the electrolyte concentration is graphically represented in *Figs.* 7 and 8. The logarithmic values of β_3 and X_3/α_3 are plotted against the electrolyte concentration in *Figs.* 9 and 10. Approximately linear relationships between ln β_3 and the electrolyte concentration appear to exist at the sodium chloride concentration from 0.1 up to 1.0 meq./100 ml indicating that β_3 increases roughly in exponential manner with the electrolyte concentration (*Fig.* 9). The quantity $\ln(X_3/\alpha_3)$ increases first, though not as fast as β_3, then seems to attain a constant value (*Fig.* 10).

Effect of Electroytes on the Rheological Behavior The following relation holds at the maximum of a V_R *vs.* κ curve[5] (*Fig.* 4):

$$\kappa=\frac{1}{2d} \tag{7}$$

Introducing d=100Å into Eq. (7) gives $\kappa=5\times10^5$ cm^{-1}. Here the d value (100 Å) represents a shorter range of the typical lengths (100–1000 Å) of a side of a bentonite platelet.[1,2] Notably, the minimum for the NaCl containing suspension (*Fig.* 2) occurs at 0.1 meq./100 ml ($n=6.02\times10^{17}$ ions/cc.). The minimum appears when the V_R is a maximum or the net interaction energy is minimum. Using the above value of n, κ was calculated from Eq. (2) for $T=300°K$, $\epsilon=80$ and $\nu=1$, and was found to be 1×10^6 cm^{-1}. It is interesting to note that the κ value thus calculated agrees reasonably well with that estimated from Eq. (7). This seems to suggest that the point of minimum viscosity is indeed where the repulsive potential is maximum. On addition of a small amount of electrolyte, V_R increases as one sees from *Fig.* 4 until κ, which is proportional to $n^{\frac{1}{2}}$ [Eq. (2)], reaches the value of $1/2d$ at which the maximum of V_R appears [see Eq. (7)]. Thus, in this region of κ (0 to $1/2d$), the addition of electrolyte introduces the decrease in the net interaction potential (V_R+V_A). This should lead to a decrease in the intrinsic relaxation time β_3 (*Fig.* 7). Similarly, the subsequent increase in β_3 is the results of decrease in V_R or the increase in the net interaction potential with further addition of the electrolyte.

The quantity β_3 is defined as;

$$\beta_3=\left[\frac{\lambda}{\lambda_1}2k'\right]_3^{-1}=\left[\frac{\lambda}{\lambda_1}2\frac{kT}{h}e^{-\Delta F^*/RT}\right]_3^{-1} \quad (8)$$

where λ and λ_1 are the molecular dimensions entering into the theory of viscosity,[6] k' is the rate of jumping of a flow unit, and ΔF^* is the Gibbs activation free energy for the jumping. Let ΔF_0^* be the activation free energy when no electrolyte is added. The activation free energy for an electrolyte-containing system, ΔF^* can be expressed by

$$\Delta F^*=\Delta F_0^*\pm c\,C_{elect} \quad (9)$$

where C_{elect} is the electrolyte concentration, and c, a constant. Combining Eqs. (8) and (9) gives

$$\beta_3=\beta_3^\circ\exp(\pm c\,C_{elect}/RT) \quad (10)$$

where β_3° is the intrinsic relaxation time when no electrolyte is added, and the minus sign is used in the concentration range lower than 0.1 meq./100 ml. At concentrations higher than the latter, the plus sign is used. Equation (10) seems to describe the approximately linear relationship between ln β_3 and C_{elect} over the high concentration range (*Fig.* 9). Because of insufficient amount of data over the low concentration range, a definite relationship between ln β_3 versus C_{elect} has not been established in this work.

It is seen in *Fig.* 7 that X_3/α_3 changes similarly with the electrolyte concentration as β_3. It seems unlikely that the intrinsic shear modulus ($1/\alpha_3$) of type 3 units resulting from the dissimilar charges on the faces and edges will be strongly dependent on the electrolyte concentration.[8] So it is suggested that the variation of X_3/α_3 is controlled largely by the fractional area of type 3 units (X_3).

Since Eq. (7) holds at the maximum of V_R, d can be considered independent of the electrolyte concentration at a given suspension concentration. If κ_1 is the value of κ for a monovalent cation and κ_m, that for an m-valent cation $\kappa_1=\kappa_m$ at the maximum of V_R. The following relation can be deduced from Eq. (2) at the maximum V_R:

$$\left(\frac{n_1\nu_1^2}{n_m\nu_m^2}\right)=1 \quad (11)$$

where n_1 is the number of monovalent cations

($\nu_1=1$), and n_m the number of ν_m-valent cations ($\nu_m=m$). For bivalent and trivalent cations,

$$n_2=n_1/4$$
$$n_3=n_1/9$$

Thus, one expects that for divalent cations the minimum on the η *vs.* electrolyte-concentration curve will occur at $n_1/4$ or 0.05 meq./100 ml whereas it appears at 0.03 meq./100 ml for trivalent cations. The limited amount of data on multivalent cations and the experimental errors inherent to the low-range of electrolyte concentration, however, did not assert a possible occurrence of the minimum (*Fig.* 2).

Let us consider the maximum in the η *vs.* C_{elect} curve (*Fig.* 2). In this work, it was uncertain whether the maximum would appear in the bentonite suspension containing NaCl (*Fig.* 2). According to a recent research on the effect of electrolyte for Veegum suspension,[9] however, the maximum appeared also in the system containing NaCl when the latter concentration was sufficiently larger than that for multivalent cations which also produced the maximum η. Thus, the appearance of maximum in the η *vs.* C_{elect} curve seems to be a general nature. It is explained by the DLVO theory for colloidal stability as follows:

The increase in η before the maximum (*Fig.* 2) is due to the increase in interaction (*i.e.*, decrease in V_R) between two particles with increasing C_{elect}. We shall call this phenomenon the DLVO effect. It may be assumed that when the interaction reached an optimum value, flocculation will occur to make platelet particles detached from the cardhouse. This would explain the maximum and the subsequent decrease in η at higher C_{elect}. We call this effect the coagulation effect. According to the DLVO theory of colloidal stability, the amounts of Na^+, Ca^{++} and Al^{+++} required to coagulate a lyophobic suspension are approximately in the ratios $1:(1/2)^6:(1/3)^6$ or $100:1.6:0.13$, in agreement with the order predicted by Schulze-Hardy rule. This explains why we could not find a maximum in our experiment with Na^+.

In our experiment (*Fig.* 2), Ca^{++} and Al^{+++} behaved similarly in a curve of η *vs.* C_{elect}. This is explained as follows:

Concerning the coagulation effect, Al^{+++} will be more effective than Ca^{++}. Thus the decrease in η will be larger with Al^{+++} than with Ca^{++}. If we consider the DLVO effect, however, the increase in with Al^{+++} is larger than with Ca^{++}. Thus the two effects should cancel with each other. This seems to explain why Al^{+++} and Ca^{++}, despite their charge difference, displayed a similar viscosity-electrolyte relationship (*Fig.* 2).

The observation that the charge type of negative ions showed little effect on η *vs.* electrolyte-concentration curve (*Fig.* 3) is not surprising because the surface charge on bentonite particle is dominantly nagative. The colloidal stability of such a system will be largely determined by the positive counter ions as predicted by the theory.[5]

Acknowledgment

One of the authors (K. Park) thanks Dr. Sang Joon Hahn for valuable discussions and suggestions. The financial support for this work was given by the National Science Foundation of the United States Government.

References

(1) R. E. Grim, "Applied Mineralogy", 16-20, McGraw-Hill, New York, 1962, p. 422.
(2) T. F. Bates, "Publication of the Mineral Industries Experiment Station," The Pennsylvania

State University, Circular No. 51, 1958.
(3) H. van Olphen, "An Introduction to Clay Colloid Chemistry" Interscience, New York, 1963.
(4) N. K. Mitra, A. K. Kauiraj and P. Bhaumik, *Trans. Indian Ceram. Soc.*, **29**, 48 (1970).
(5) E. J. W. Verwey and J. Th. G. Overbeek, "Theory of the Stability of Lyophobic Colloids," Elsevier, Amsterdam, 1948, p. 205.
(6) T. Ree and H. Eyring, "Rheology," ed. by F. R. Eirich, Vol. II, p. 83, Academic Press, New York, 1958, p. 591; *J. App. Phys.* **26**, 793, 800 (1955).
(7) H. Utsugi, K. Kim, T. Ree, and H. Eyring, *NLGI Spokesman* (J. National Lubricating Grease Institute), **25**, 125 (1961).
(8) K. Park and T. Ree, *J. Korean Chem. Soc.*, **15**, 293 (1971).
(9) K. P. Lee, R. C. Mason and T. Ree, *J. Korean Chem. Soc.*, in press.

DAEHAN HWAHAK HWOEJEE
(Journal of the Korean Chemical Society)
Vol. 15, Number 6, 1971
Printed in Republic of Korea

오르토 치환 아닐린과 요오드 사이의 착물에 관한 연구

이부영 · 최상업
서강대학교 이공대학 화학과

(1971. 10. 7 接受)

The Complexes of Iodine with Ortho-Substituted Anilines in Carbon Tetrachloride*

Bu Yong Lee and Sang Up Choi**
Department of Chemistry, Sogang University, Seoul.

(Received Oct. 7, 1971)

요 약 아닐린, *o*-톨루이딘, *o*-에틸아닐린, *o*-클로로아닐린등과 I_2 사이의 상호작용을 자외선 분광광도법으로 조사한 결과 CCl_4 용액내에서 아닐린 또는 상기 *o*-치환 아닐린과 I_2 사이에 1 : 1 착물이 형성됨을 알았다. 이들 착물의 실온에서의 형성상수를 구한 결과 다음과 같은 값을 얻었다. $C_6H_5NH_2 \cdot I_2$, 12.8 l mole^{-1}; *o*-$CH_3C_6H_4NH_2 \cdot I_2$, 9.31 l mole^{-1}; *o*-$C_2H_5C_6H_4NH_2 \cdot I_2$, 3.15 l mole^{-1}; *o*-$ClC_6H_4NH_2 \cdot I_2$, 0.576 l mole^{-1}. 본실험결과를 전 실험의 결과와 비교하면 I_2 · 아민 착물의 안정도가 다음 순으로 감소함을 알 수 있다

$C_6H_5N(C_2H_5)_2 > C_6H_5N(CH_3)_2 > C_6H_5NH_2 > o\text{-}CH_3C_6H_4NH_2 > o\text{-}C_2H_5C_6H_4NH_2 > o\text{-}ClC_6H_4NH_2$

이들 착물의 상대적 안정도는 치환기의 유발효과와 입체효과에 의하여 설명될 수 있다.

Abstract The interactions of aniline, *o*-toluidine, *o*-ethylaniline and *o*-chloroaniline with iodine in carbon tetrachloride solution have been examined through spectrophotometric measurements. The results indicate that both aniline and the *o*-substituted anilines examined form one-to-one complexes with I_2 in solution. The formation constants of the complexes measured at room temperature are 12.8, 9.31, 3.15 and 0.576 l mole^{-1}, respectively. Comparison of these results with previous experimental results indicates that the relative stabilities of the I_2-amine complexes decrease in the

* The Molecular Complexes. X.
** Department of Agricultural Chemistry, Jinju Agricultural College, Jinju.